Parallel and Decoupled XY Flexible Positioning Platform for Micro LED Panel Repair

1st Wenxiu Lai
State Key Laboratory of Precision Electronic Manufacturing Equipment and Technology, Guangdong University of Technology
School of Electromechanical Engineering, Guangdong University of Technology
Guangzhou, China
623118907@qq.com

2nd Jian Gao*
State Key Laboratory of Precision Electronic Manufacturing Equipment and Technology, Guangdong University of Technology
School of Electromechanical Engineering, Guangdong University of Technology, Guangzhou, China
Corresponding author :
jian_gao2004@163.com

3rd Lanyu Zhang
State Key Laboratory of Precision Electronic Manufacturing Equipment and Technology, Guangdong University of Technology
School of Electromechanical Engineering, Guangdong University of Technology
Guangzhou, China
lyuzhang@qq.com

4th Yongbin Zhong
State Key Laboratory of Precision Electronic Manufacturing Equipment and Technology, Guangdong University of Technology
School of Electromechanical Engineering, Guangdong University of Technology
Guangzhou, China
yongb_z@163.com

***Abstract*—In the field of microelectronics packaging, microled mass transferring technology has become the key for manufacturing of large-scale display panel, and the defect repair technology is particularly important for the quality control of the display panel. In general, this repair process requires the motion mechanism to reach and replace the defective chip target in a high-speed and high positioning precision for the entire panel. In order to meet the requirements of MicroLED panel repair, this paper introduces an XY parallel decoupling flexible micro-motion platform for the large-stroke macro-micro composite stage. The flexible platform is guided by two pairs of flexible double bridge amplifying mechanisms, which are distributed symmetrically around the moving platform. The mobile pair, which is spliced by S-type hinges, is connected to the moving platform to achieve the performance of decoupling input and output. Based on the micro stage structure, the flexibility and stiffness analysis are performed through static and dynamic modeling of the flexible platform. The particle swarm optimization method is used for size optimization and mechanism modeling. The performance of the micro-motion stage was verified by finite element simulation analysis. The simulation results show that the XY flexible platform proposed in this paper has good parallel decoupling and amplification ratio, and can be used to develop the macro-micro motion stage for defect repair of MicroLED panel.**

Keywords—Micro LED, precision repair, macro-micro motion platform, nano-positioning platform, flexible hinge

I. INTRODUCTION

In recent years, the new generation of display panel leader micro LED has become the focus of microelectronic packaging field. Compared with traditional LCD and OLED display technology, it does not need to rely on backlight, has longer service life, higher color saturation, and can achieve seamless splicing and other advantages [1]. In the past, it was generally believed that the biggest bottleneck of micro led was mass transfer technology. However, with the advent of mass transfer schemes [2] such as pick & place transfer, fluid assembly, laser transfer and roller transfer, the focus of the bottleneck gradually shifted to micro LED panel repair.

It takes about 25 million LED chips to achieve a 55 inch 4K resolution display with micro LEDs. Even if the transfer yield is 99.99% and the accuracy of each chip is controlled within plus or minus 0.5 μm , 2500 defective chips may exist in a single panel. Therefore, the pixel defect repair technology of large panel is particularly important for quality control. The repair process of this defect needs to achieve high-speed and high positioning accuracy in the large panel area, so it needs a motion platform with large motion range, high-speed and high-precision. Unfortunately, the traditional rigid mechanism has some shortcomings such as friction, clearance and assembly error, so it is difficult to meet the requirements of high precision in performance. However, compared with the traditional rigid mechanism, the compliant mechanism relies on its own elastic deformation to transfer motion, force and energy, which has the advantages of simple structure, no gap, no friction and high motion accuracy. Therefore, compliant mechanism has become a promising choice in precision positioning platform.

At present, XY motion platform can be divided into series structure and parallel structure. The second axis motion is overlapped [3] or inlaid [4] in the first axis motion stage by the way of orthogonal in series structure. The structure design is relatively simple and it is easy to obtain the positive kinematics solution, but there are some shortcomings such as serious accumulated error, large inertia and low natural frequency. On the contrary, although the design and optimization of parallel structure is more complex and challenging, it has compact structure, high rigidity, high precision and better bearing capacity [5]. Therefore, parallel structure becomes a good choice for the design of micro nano positioning platform.

In order to meet the requirements of micro LED panel repair, a large stroke cross scale macro micro composite motion platform structure is proposed. The XY parallel decoupled flexible positioning micro motion platform is mainly introduced. The flexible positioning platform is driven by piezoelectric ceramic, combined with the double bridge amplification mechanism [6] designed by V-type flexible hinge, to achieve large stroke and high rigidity. The whole platform is designed symmetrically with mirror surface, and the mobile pair is spliced by S-shaped hinge to connect the mobile platform, so as to realize the work requirements of input and output decoupling. Based on the flexibility matrix method, XY flexible platform is statically modeled, and based on the Lagrange energy method, XY flexible platform is dynamically modeled. The performance of the designed fretting platform is verified by ANSYS simulation.

The rest of the paper is as follows: Section II introduces the structural design of the platform, statics and dynamics modeling of the mechanism are carried out in Section III, and the performance of the designed fretting platform is verified by ANSYS simulation analysis in section IV. finally, a brief conclusion is made in section V.

II. MECHANISM DESIGN

Based on the macro platform, this paper designs a XY decoupling micro positioning platform with large stroke, high speed and high precision. In the actuator, piezoelectric ceramic is selected. It has the advantages of compact structure, high resolution of motion, large output force, high efficiency of energy conversion, no mechanical loss, no magnetic field, fast response and so on. It is widely used in various precision equipment. However, the stroke of piezoelectric actuator is small, so in order to achieve the requirement of large stroke, micro displacement amplification mechanism is needed to achieve the amplification and transmission of piezoelectric output displacement. Compared with single bridge amplifying mechanism [7] and lever amplifying mechanism [8], the amplifying mechanism adopts double bridge amplifying mechanism, which has higher lateral stiffness and can guarantee linear output motion, and also plays the role of decoupling and motion guidance in the whole motion platform. The double bridge micro displacement amplification mechanism realizes the micro motion transmission without friction and clearance through the elastic deformation of flexible hinge, and then realizes the displacement amplification of piezoelectric stack. In this paper, V-shaped flexure hinge is used. When the radius r of V-shaped flexure hinge is equal to $l/4$ and the angle is equal to $\pi/4$, it has higher rigidity than the circular and leaf flexure hinge [9].

In this paper, the 4-PP decoupling structure is established by using the orthogonal 2-PP parallel kinematic configuration. P represents the flexible moving pair, which not only transfers the force, but also transfers the displacement. Its transfer characteristics directly affect the static and dynamic working characteristics of the positioning platform. The double four-bar moving pair, which is spliced by S-type hinge [10], has greater flexibility and no displacement loss. The whole structure adopts mirror symmetrical design, which can balance the internal stress of the system, improve the rigidity and bearing characteristics of the center moving platform, and effectively avoid the influence of the coupling movement and temperature drift between dimensions [11]. In order to improve the dynamic performance of precision motion platform, materials with high Young's modulus E to low density ratio ρ are needed, because the materials with high stiffness and light weight can increase the stiffness and bandwidth of motion platform. In this study, al7075 is selected to manufacture precision motion platform, and the detailed parameters are shown in Table I.

TABLE I. THE PARAMETERS OF THE AL7075

Young's modulus	*Yield strength*	*Poisson's ratio*	*Density*
71.7GPa	503MPa	0.33	$2.81\times10^3 Kg/m^3$

III. PREPARE YOUR PAPER BEFORE STYLING

There are many modeling methods for compliant mechanisms, including pseudo rigid body modeling, nonlinear modeling and flexibility modeling. The flexibility matrix method is based on Hooke's law to calculate the flexibility of the flexure hinge in all directions, which is more efficient. In order to establish a more accurate model, this paper uses the flexibility matrix method to solve the kinematic static model of the platform.

In this paper, two-dimensional XY micro positioning platform is studied. According to the mechanics of materials, the displacement load relationship of the free end of the flexure hinge is

$$\begin{Bmatrix}\Delta x\\ \Delta y\\ \Delta\theta\end{Bmatrix}=\begin{bmatrix}C_{x,F_x} & 0 & 0\\ 0 & C_{y,F_y} & C_{y,M_z}\\ 0 & C_{\theta,F_y} & C_{\theta,M_z}\end{bmatrix}\begin{Bmatrix}F_x\\ F_y\\ M_z\end{Bmatrix} \quad (1)$$

Among them, from the reciprocity principle $C_{y,M_z}=C_{\theta,F_y}$; Δx , Δy and $\Delta\theta$ are the displacements of the flexure hinge along, x,y and z axis respectively; F_x , F_y and M_z are the loads acting on the flexure hinge end along, x,y and z axis respectively; C is the flexibility coefficient.

The flexibility matrix C_i under the local coordinate system O_i of flexure hinge is transformed into the flexibility matrix C_j under different coordinate systems O_j by coordinate transformation, and the conversion formula is

$$C_i^j = T_i^j C_i (T_i^j)^T \quad (2)$$

Where T_i^j is the homogeneous coordinate transformation matrix, and

$$T_i^j = \begin{bmatrix} R_i^j & S\left(r_i^j\right) R_i^j \\ 0 & R_i^j \end{bmatrix} \quad (3)$$

In general, compliant mechanisms are constructed by a number of flexible hinges and rigid connection ends in series or parallel. In order to obtain the stiffness model of the whole mechanism, it is necessary to convert the local flexibility of all flexure hinges into the global flexibility. The flexibility of the whole mechanism can be obtained by adding the flexibility of series connection and the stiffness of parallel connection. The flexibility of series and parallel mechanisms can be expressed as

$$C_0 = \sum_{i=1}^{k} T_{0_i}^{0} C_{0_i} (T_{0_i}^{0})^T \quad (4)$$

$$C_0 = \left(\sum_{i=1}^{k} \left(T_{0_i}^{0} C_{0_i} (T_{0_i}^{0})^T \right)^{-1} \right)^{-1} \quad (5)$$

Tian proposed a V-shaped flexible hinge with fillet, which has a large compliance range, corresponding to different fillet radius R and angle, and established its flexibility matrix as C_v , and its geometric parameters are shown in Fig. 1(a). When the fillet radius R is equal to $l/4$ and the angle is equal to $\pi/4$, the V-shaped flexure hinge has higher rigidity than the right semicircle and blade flexure hinge.

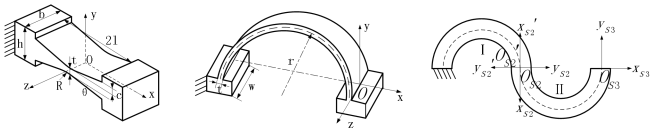

Fig. 1. Geometric parameters of v-hinge (a) and geometric parameters of semi-circular beam hinge (b) and geometric parameters of s-hinge(c).

There are mature research conclusions on the flexibility characteristics of semicircle beams. In this paper, the flexibility matrix of semicircle beams is established as C_c by using the method given by Yuan et al. And its geometric parameters are shown in Fig. 1(b). A complete S-type flexure hinge is composed of two semi-circular beams with rectangular section in series, and its geometric parameters are shown in Fig. 1(c). By linear superposition of two semi-circular curved beams, the flexibility matrix of S-type flexure hinge is established as

$$C_s = T_{S2}^{S3} R_{S2}^{S3} C_c \left(R_{S2}^{S3} \right)^T \left(T_{S2}^{S3} \right)^T + T_{S2'}^{S3} R_{S2'}^{S3} C_c \left(R_{S2'}^{S3} \right)^T \left(T_{S2'}^{S3} \right)^T \quad (6)$$

A. Output Compliance Modeling

1) Output Compliance of Displacement Amplifier

Due to the double symmetry of the parallel mechanism, the kinematic branch chain C is taken as an example for analysis. The composite bridge amplifying mechanism is a symmetrical mechanism, and the 1/4 structure is selected as the research object, as shown in Fig. 2(a). Due to the series connection, the compliance matrix of point B relative to points O_1 and O_5 is

$$C_B^1 = T_2^B C_2 \left(T_2^B \right)^T + T_4^B C_4 \left(T_4^B \right)^T \quad (7)$$

$$C_B^5 = T_6^B C_6 \left(T_6^B \right)^T + T_8^B C_8 \left(T_8^B \right)^T \quad (8)$$

Among them, the flexibility of the flexible hinge $C_i = C_v$ (i=2,4,6,8).

In view of the compound bridge amplifier O_1O_4 and O_5O_8 the two flexible chains are connected in parallel, so the output flexibility matrix of its 1/4 mechanism is

$$C_B^A = \left(K_B^A \right)^{-1} = \left(K_B^1 + K_B^5 \right)^{-1} = \left[\left(C_B^1 \right)^{-1} + \left(C_B^5 \right)^{-1} \right]^{-1} \quad (9)$$

Since the left half of the bridge amplifier is symmetrical from top to bottom, the flexibility matrix of the lower half of the left half can be obtained by rotating the X axis by 180 degrees. The flexibility matrix of the left half of the bridge amplifier is

$$_1C_B = T_d^u (C_B^A) (T_d^u)^T + C_B^A \quad (10)$$

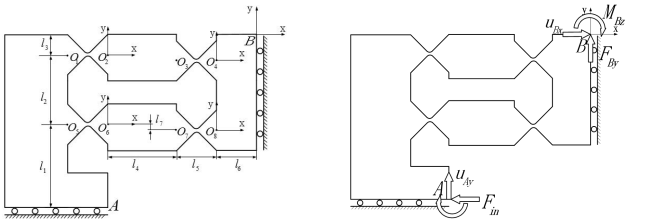

Fig. 2. 1/4 model of composite bridge mechanism (a) and stress analysis(b).

Since the composite bridge amplifying mechanism is bilaterally symmetrical, the flexibility matrix on the right half can be obtained by rotating the Y axis by 180 degrees, then the output flexibility of the entire composite bridge amplifying mechanism is

$$_AC_B = \left(K_B \right)^{-1} = \left[\left(_1C_B \right)^{-1} + \left(_rC_B \right)^{-1} \right]^{-1} = \left[\left(_1C_B \right)^{-1} + \left(T_r^l \left(_1C_B \right) \left(T_r^l \right)^T \right)^{-1} \right]^{-1} \quad (11)$$

2) Output Compliance of XY stage

The double parallel four-bar mechanism is bilaterally symmetrical. The left half of the single parallel four-bar is composed of two branch chains. Each branch chain is formed by an S-shaped flexible hinge connected in series. 1/2 of the double four-bar moving pair is selected as the research object As shown in Fig 3. The flexibility matrix of S-shaped flexible branches is

$$C_C^9 = \sum_{i=10}^{k} T_i^C C_i \left(T_i^C \right)^T \quad (12)$$

$$C_C^{15} = \sum_{i=16}^{k} T_i^C C_i \left(T_i^C \right)^T \quad (13)$$

$$_1C_{sp1} = \left(K_C^9 + K_C^{15} \right)^{-1} = \left[\left(C_C^9 \right)^{-1} + \left(C_C^{15} \right)^{-1} \right]^{-1} \quad (14)$$

Among them, the flexibility of the flexible hinge $C_i = C_s$ (i = 10, 11, 12, 13, 14, 16, 17, 18, 19, 20).

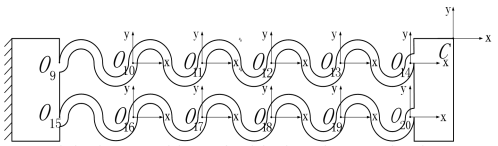

Fig. 3. 1/2 model of S-type hinge double four-bar mechanism.

The compliance matrix of the single parallel four-bar mechanism on the right half can be obtained by rotating the Y axis by 180 degrees, then the compliance matrix of the S-shaped moving pair is

$$C_{sp1} = \left[\left(_1C_{sp1} \right)^{-1} + \left(_rC_{sp1} \right)^{-1} \right]^{-1} = \left[\left(_1C_{sp1} \right)^{-1} + \left(T_r^l \left(_1C_{sp1} \right) \left(T_r^l \right)^T \right)^{-1} \right]^{-1} \quad (15)$$

The double-bridge amplifying mechanism in the XY micro platform is connected in series with the double parallel four-bar mechanism first, and then connected in series with the moving platform through the double parallel four-bar mechanism. The one-dimensional output flexibility of the XY micro platform is

$$C_0 = C_C = T_{sp2}^0 C_{sp2} \left(T_{sp2}^0 \right)^T + T_{sp1}^0 C_{sp1} \left(T_{sp1}^0 \right)^T + T_B^0 {}_A C_B \left(T_B^0 \right)^T \quad (16)$$

The XY two-dimensional micro-platform is composed of four branch chains of C, D, E, and F. D and F constitute the branch chain of X-axis movement, and C and E constitute the branch chain of Y-axis movement. The output flexibility

matrix of the four branches of C, D, E, and F on the XY translation micro-motion stage at point O is

$$C_{Oo} = \left[\left(C_C\right)^{-1} + \left(T_E^O C_C \left(T_E^O\right)\right)^{-1} + \left(T_F^O C_C \left(T_F^O\right)\right)^{-1} + \left(T_G^O C_C \left(T_G^O\right)\right)^{-1} \right]^{-1} \quad (17)$$

B. Input Stiffness Modeling

When the input force Fin is applied, the input end stiffness KA should not exceed the output stiffness of the piezoelectric ceramic. When the double-bridge amplifying mechanism B in the branch chain C is connected to the branch of the XY micro-positioning platform as a decoupler, it will withstand the forces applied by the remaining three branches (D, E, F) and points B and O, As shown in Figure 4. The compliance matrix except the double-bridge micro-displacement amplification mechanism is

$$C_B = \left(K_B^O\right)^{-1} + T_O^B \left({}_{chainDEF}K_O\right)^{-1} \left(T_O^B\right)^T \quad (18)$$

In the formula, ${}_{chainDEF}K_O$ is the equivalent rigidity of the flexible branch with respect to point O.

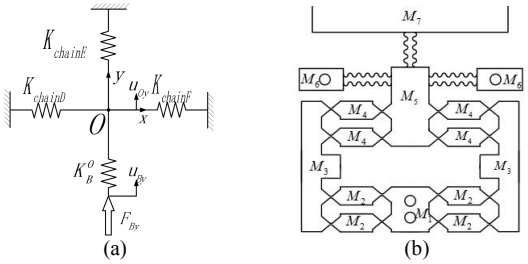

Fig. 4. Rigidity model of XY micro platform(a) and XY micro platform 1/4 structure dynamic model.

The force situation of 1/4 of the double-bridge micro-displacement amplifying mechanism is shown in Fig. 2(b). Assuming that the output B point is fixed, the static equilibrium equation obtained according to (1) is

$$u_{in} = c_{11}F_{in} + c_{12}F_{By} + c_{13}M_{Bz} \quad (19)$$

$$u_{By} = c_{21}F_{in} + c_{22}F_{By} + c_{23}M_{Bz} \quad (20)$$

$$\theta_{Bz} = c_{31}F_{in} + c_{32}F_{By} + c_{33}M_{Bz} \quad (21)$$

In the formula, Fin is the external load received by the mechanism, F_{By} represents the force applied by the XY platform in the y direction, M_{Bz} is the equivalent bending moment at the output B point; u_{in} is the displacement of the input A point along the x axis, u_{By} Is the displacement of point B at the output along the y axis, θ_{Bz} is the rotation angle of point B at the output about the z axis is equal to 0, c_{ij} (i, j = 1,2,3) is the flexibility of the composite bridge type 1/4 amplification mechanism Elements of matrix C_B^A.

In addition, the displacement u_{By} and acting force F_{By} of point B along the y axis also satisfy the following relationship in the overall compliance matrix

$$u_{By} = -b_{22}F_{By} \quad (22)$$

In the formula, $b_{22} = C_B$ (2,2). According to (19) to (22), u_{in}, F_{By}, M_{Bz}, u_{By} can be obtained, so that the input flexibility of the two-dimensional operating platform can be obtained as

$$C_{in} = \frac{c_{22}c_{33} - c_{23}c_{32} + b_{22}c_{33}}{c_{11}\left(c_{22}c_{33} - c_{23}c_{32}\right) + c_{12}\left(c_{23}c_{31} - c_{21}c_{33}\right) + c_{13}\left(c_{21}c_{32} - c_{22}c_{31}\right) + b_{22}\left(c_{11}c_{33} - c_{13}c_{31}\right)} \quad (23)$$

From (19) to (23), the magnification ratio of the compound bridge micro-displacement amplifying mechanism can be derived as

$$A_a = \frac{u_{By}}{u_{in}} = \frac{b_{22}\left(c_{21}c_{33} - c_{23}c_{31}\right)}{C_{in}\left(c_{22}c_{33} - c_{23}c_{32} + C_{22}c_{33}\right)} \quad (24)$$

C. Amplification Ratio Deviation

Since the forces F_{By} in the y direction at points O and B are equal, the output displacement of point O at the center of the moving platform is

$$u_{Oy} = \frac{a_{22}}{b_{22}} u_{By} \quad (25)$$

In the formula, $a_{22} = {}_{chainDEF}C_O(2,2)$.

Therefore, according to (19) to (25), the formulas of the output displacement and displacement magnification ratio of the XY micro-positioning platform can be obtained as

$$u_{Oy} = \frac{a_{22}b_{22}\left(c_{21}c_{33} - c_{23}c_{31}\right)}{b_{22}\left(c_{22}c_{33} - c_{23}c_{32} + b_{22}c_{33}\right)} F_{in} \quad (26)$$

$$A = \frac{a_{22}b_{22}\left(c_{21}c_{33} - c_{23}c_{31}\right)}{b_{22}\left[c_{11}\left(c_{22}c_{33} - c_{23}c_{32}\right) + c_{12}\left(c_{23}c_{31} - c_{21}c_{33}\right) + c_{13}\left(c_{21}c_{32} - c_{22}c_{31}\right) + b_{22}\left(c_{11}c_{33} - c_{13}c_{31}\right)\right]} \quad (27)$$

D. Dynamics Model

In this paper, the Lagrange method is used to establish the dynamic model of the XY micro-positioning platform. The input displacement variable d = [q1, q2] T is selected as the generalized coordinates, so the kinetic energy and potential energy of the compliant mechanism can be expressed in generalized coordinates. It is assumed that the kinetic energy is generated by the rigid beam connected to the flexible hinge, and the potential energy is introduced through the elastic deformation of the flexible hinge. Since the XY micro-positioning platform is placed horizontally, the gravitational potential energy can be ignored.

$$T_C = \frac{1}{2}m_2\left(\frac{\dot{q}_1^2}{4} + \frac{\dot{q}_2^2}{16}\right) + \frac{1}{2}m_3\left(\dot{q}_1^2 + \frac{\dot{q}_2^2}{4}\right) + \frac{1}{2}m_4\left(\frac{\dot{q}_1^2}{4} + \frac{9\dot{q}_2^2}{16}\right) + \frac{1}{2}m_5\dot{q}_2^2 + \frac{1}{24}\left(m_2 + m_4\right)\left(l_4^2 + 3(l_4 + 2l_5)^2\right)\dot{\theta}_1^2 \quad (28)$$

$$T_D = \frac{1}{2}m_2\left(\frac{\dot{q}_2^2}{4} + \frac{\dot{q}_1^2}{16}\right) + \frac{1}{2}m_3\left(\dot{q}_2^2 + \frac{\dot{q}_1^2}{4}\right) + \frac{1}{2}m_4\left(\frac{\dot{q}_2^2}{4} + \frac{9\dot{q}_1^2}{16}\right) + \frac{1}{2}m_5\dot{q}_1^2 + \frac{1}{24}\left(m_2 + m_4\right)\left(l_4^2 + 3(l_4 + 2l_5)^2\right)\dot{\theta}_2^2 \quad (29)$$

According to the symmetrical structure of the XY platform, the kinetic energy of branch E and branch F are $T_C=T_E$ and $T_D=T_F$, respectively.The kinetic energy of the motion platform is

$$T_O=\frac{1}{2}m_7\dot{q}_1^{\,2}+\frac{1}{2}m_7\dot{q}_2^{\,2} \tag{30}$$

Therefore, the total kinetic energy of the entire platform is

$$T=\left(\frac{5}{16}m_2+\frac{5}{4}m_3+\frac{13}{16}m_4+\frac{1}{12}\frac{m_4\left(l_4^{\,2}+3(l_4+2l_5)^2\right)}{4\left(l_4+l_5\right)^2+l_7^2}+\frac{1}{2}m_7+m_5\right)\dot{q}_1^2$$
$$+\left(\frac{5}{16}m_2+\frac{5}{4}m_3+\frac{13}{16}m_4+\frac{1}{12}\frac{m_4\left(l_4^{\,2}+3(l_4+2l_5)^2\right)}{4\left(l_4+l_5\right)^2+l_7^2}+\frac{1}{2}m_7+m_5\right)\dot{q}_2^2 \tag{31}$$

In equations (28) to (31), m_2,m_3,m_4,m_5,m_7 is the mass of the rigid link and platform respectively and $q_2=Aq_1$.

Based on the principle of virtual work, the total potential energy of the XY flexible micro-platform is

$$U=\frac{1}{2}K_{inX}q_1^{\,2}+\frac{1}{2}K_{inY}q_2^{\,2} \tag{32}$$

In the formula, K_{inX} and K_{inY} are the input stiffness of X axis and Y axis respectively.

Therefore, the kinetic energy and potential energy of the system can be written as independent functions with q_1 as the variable, and substituted into the Lagrange equation

$$\frac{d}{dt}\left(\frac{\partial T}{\partial\dot{q}_j}\right)-\frac{\partial T}{\partial q_j}+\frac{\partial V}{\partial q_j}=Q_j,\ (\mathrm{j}=1,2,\cdots,\mathrm{k}) \tag{33}$$

In the formula, Q_i is the driving force.

The undamped free vibration dynamic equation of the compliant mechanism can be derived as

$$M\ddot{q}_1+K_{in}q_1=0 \tag{34}$$

In the formula, M_e is the equivalent mass of the micro platform, and K_e is the equivalent rigidity of the micro platform.

According to the vibration theory, the modal equation of the undamped free vibration characteristic of the compliant mechanism can be obtained as

$$\left(K_{in}\text{-}M_i\lambda_i^{\,2}\right)\phi_i=0 \tag{35}$$

From this, the first-order natural frequency of the micro-platform can be obtained as

$$f_i=\frac{1}{2\pi}\lambda_i=\frac{1}{2\pi}\sqrt{\frac{K_{in}}{M}} \tag{36}$$

IV. FEA ANALYSIS AND EVALUATION

In order to verify the performance of the XY flexible micro-positioning platform, ANSYS Workbench software was used for finite element analysis. Using the size parameters listed in Table II, the Solidworks software was used to construct a three-dimensional model of the XY flexible micro-positioning platform, set the parameters of the material Al7075 shown in Table I, and import ANSYS Workbench to establish a finite element model. Intelligent meshing and zooming are used for meshing. The static analysis and modal analysis process are described below.

TABLE II. THE PARAMETERS OF AN XY STAGE (mm)

w	*r1*	θ	*b*	*l*	*r2*	*c*
15	1.05	45	1	4.2	16.27	3.765
l1	***l2***	***l3***	***l4***	***l5***	***l6***	***l7***
16.27	15.03	4.44	24	8.4	11	3

A. Kinematics Analysis

In order to test the amplification and decoupling performance of the XY flexible parallel micro-platform, the deformation relationship and performance are evaluated as follows by applying a driving force. When a driving force of 200N is applied to the input, the maximum deformation occurs on the intermediate platform, and the maximum coupling error is 0.0012%. A group of input displacements of 10um, 20um, 40um, 60um and 80um are simultaneously applied on the input end. As shown in Table III and Figure 5, the magnification ratio is 4.2. It can be observed that the value of the displacement magnification is not affected by the input displacement, and the displacement magnification is not affected by this. The error from the theoretical magnification ratio is 15.01%.

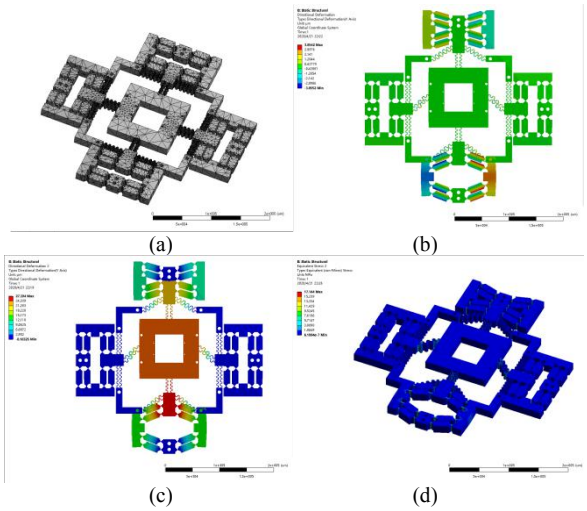

Fig. 5. FEA Static structural analysis results.

TABLE III. THE PERFORMANCES OF AN XY STAGE

δ_{in}/*um*	δ_{out}/*um*	$\sigma_{\max}$/*MPa*	*A*	*Error/%*
10	83.92	59.99	4.2	0.0012
20	167.84	120	4.2	0.0012
40	335.69	239.99	4.2	0.0012
60	503.53	359.99	4.2	0.0012
80	671.38	479.98	4.2	0.0012

In order to evaluate the accuracy, when a set of forces from 200N to 2400N are applied to the input terminal in the X direction, the results are shown in Table IV. With the increase of the driving force, all the displacements of the key points Both increase at a constant rate, and the relationship between the output displacement and the input force is linear, which indicates that there is no stiffness nonlinear effect in

the compliant mechanism. In addition, the XY flexible micro-positioning platform has the potential to withstand input forces of up to 2400 N, where the maximum equivalent stress is 207.61 MPa and there is no material damage.

TABLE IV. THE OUTPUT DISPLACEMENT IN TERMS OF THE VARIATION OF THE INPUT FORCE

F/N	δ_{out} */um*	σ_{max} */MPa*	*A*	*Error/%*
200	23.978	17.14	4.2	0.0012
400	47.957	34.29	4.2	0.0012
600	71.933	51.91	4.2	0.0110
800	95.91	69.20	4.2	0.0110
1000	119.89	86.51	4.2	0.0110
1400	167.84	121.11	4.2	0.0110
1800	215.8	155.72	4.2	0.0110
2400	287.73	207.61	4.2	0.0110

B. *Modal Analysis*

The dynamic performance of the XY flexible micro-positioning platform is further verified through modal analysis. ANSYS extracts the first six modes of the model. As shown in Figure 6, red represents the maximum displacement and blue represents the minimum displacement. Because the structure is completely symmetrical, the first-order and second-order deformations occur along the X and Y axes, respectively, and their resonance frequencies are very close to 181.29 Hz and 184.22 Hz, respectively, and have higher operating frequencies. Rotational deformation occurs in the third order, and its resonance frequency is 220.83 Hz. The fourth, fifth, and sixth resonance frequencies are 306.85 Hz, 421.42 Hz, and 422.52 Hz, respectively. Obviously, the XY flexible micro-positioning stage expects to produce translational motion along the X and Y axes. Therefore, the first two natural frequencies of the platform are critical to the overall positioning performance. All finite element analysis results confirm that the proposed XY flexible micro-platform has excellent performance in performing high-performance precision positioning.

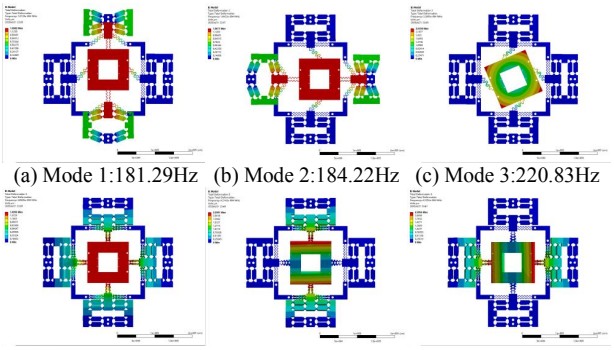

(a) Mode 1:181.29Hz (b) Mode 2:184.22Hz (c) Mode 3:220.83Hz

(d) Mode 4:306.85Hz (e) Mode 5:421.42Hz (f) Mode 6:422.52Hz

Fig. 6. Modal analysis results.

V. CONCLUSION

Addressing the difficult in repair of large scale MicroLED display panel, this paper designed an XY parallel decoupling flexible micro-positioning platform the XY flexible mechanism was described in terms of the input stiffness, output flexibility, and amplification ratio of the platform through the flexibility matrix method. Its dynamic model of the mechanism was established through the Lagrange equation. The performance of the XY micro-positioning platform was evaluated through kinematics analysis and modal analysis. The results show that the displacement amplification ratio of this mechanism can reach 4.2, the maximum output displacement can reach 0.671mm, the coupling displacement error is only 0.0012%,and the natural frequency is 181.29Hz. Therefore, the XY flexible platform proposed can achieve a good performance in parallel decoupling and magnification aspect. Further work will be carried out on the motion control and implementation of the XY parallel platform for the application of MicroLED panel repair.

ACKNOWLEDGMENT

The work presented in the paper is supported by Fund of Guangdon g R&D Science and Technology (2018B090906002).Basic and Applied Basic Research Foundation Project of Guangdong(2019A1515011796).National Natural Science Foundation of China(51905108).

REFERENCES

[1] K. Ding, V. Avrutin, N. Izyumskaya, Ü. Özgür, and H. Morkoç, "Micro-LEDs, a Manufacturability Perspective," *Applied Sciences,* vol. 9, no. 6, p. 1206, 2019.

[2] T. Wu *et al.*, "Mini-LED and Micro-LED: Promising Candidates for the Next Generation Display Technology," *Applied Sciences,* vol. 8, no. 9, p. 1557, 2018.

[3] Z. Wu and Q. Xu, "Design, optimization and testing of a compact XY parallel nanopositioning stage with stacked structure," *Mechanism and Machine Theory,* vol. 126, pp. 171-188, 2018.

[4] B. J. Kenton and K. K. Leang, "Design and Control of a Three-Axis Serial-Kinematic High-Bandwidth Nanopositioner," *IEEE/ASME Transactions on Mechatronics,* vol. 17, no. 2, pp. 356-369, 2012.

[5] G.-Q. Lu, A. Čereška, G. Augustinavičius, R. Maskeliunas, M. Ragulskis, and W.-H. Hsieh, "Intelligent control and performance evaluation of a novel precise positioning stage," *Journal of Intelligent & Fuzzy Systems,* vol. 36, no. 2, pp. 1205-1214, 2019.

[6] Z. Wu and Y. Li, "Optimal design and comparative analysis of a novel microgripper based on matrix method," presented at the 2014 IEEE/ASME International Conference on Advanced Intelligent Mechatronics: 2014 IEEE/ASME International Conference on Advanced Intelligent Mechatronics (AIM), July 8-11, 2014, Besancon, France, Besancon(FR), 2014.

[7] H. Wei, B. Shirinzadeh, W. Li, L. Clark, J. Pinskier, and Y. Wang, "Development of Piezo-Driven Compliant Bridge Mechanisms: General Analytical Equations and Optimization of Displacement Amplification," *Micromachines,* vol. 8, no. 8, p. 238, 2017.

[8] S. He *et al.*, "Development and Repetitive-Compensated PID Control of a Nanopositioning Stage With Large-Stroke and Decoupling Property", *IEEE Transactions on Industrial Electronics,* vol. 65, no. 5, pp. 3995-4005, 2018.

[9] Y. Tian, B. Shirinzadeh, and D. Zhang, "Closed-form compliance equations of filleted V-shaped flexure hinges for compliant mechanism design," *Precision Engineering,* vol. 34, no. 3, pp. 408-418, 2010.

[10] N. Wang, X. Liang, and X. Zhang, "Pseudo-rigid-body model for corrugated cantilever beam used in compliant mechanisms," *Chinese Journal of Mechanical Engineering,* vol. 27, no. 1, pp. 122-129, 2014.

[11] J. Huang and Y. Li, "Design and Analysis of a Completely Decoupled Compliant Parallel XY Micro-motion Stage," presented at the 2010 IEEE International Conference on Robotics and Biomimetics. [v.2], Tianjin, China, 2010.